SPACE MAPPING TECHNIQUE FOR ELECTROMAGNETIC OPTIMIZATION

J.W. Bandler, R.M. Biernacki, S.H. Chen,
P.A. Grobelny and R.H. Hemmers

SOS-94-6-R

March 1994

SPACE MAPPING TECHNIQUE FOR ELECTROMAGNETIC OPTIMIZATION

J.W. Bandler, Fellow, IEEE, R.M. Biernacki, Senior Member, IEEE, S.H. Chen, Member, IEEE, P.A. Grobelny and R.H. Hemmers, Student Member, IEEE

Abstract

We offer space mapping (SM), a fundamental new theory to circuit optimization utilizing a parameter space transformation. This technique is demonstrated by the optimization of a microstrip structure for which a convenient analytical/empirical model may not exist. For illustration, we focus upon a 3-section microstrip impedance transformer and a double folded stub microstrip filter utilizing an electromagnetic (EM) field simulator and explore various design characteristics. We propose two distinct EM models: coarse for fast computations, and the corresponding fine for a few more accurate and necessary simulations. The coarse model, useful when circuit-theoretic models may not be readily available, permits rapid exploration of different starting points, solution robustness, local minima, parameter sensitivities, yield-driven design and other design characteristics within a practical time frame. The computationally expensive fine model is used to verify the space-mapped designs obtained exploiting the coarse model, as well as in the SM process itself.

J.W. Bandler, R.M. Biernacki and S.H. Chen are also with Optimization Systems Associates Inc., P.O. Box 8083, Dundas, Ontario, Canada L9H 5E7.

This work was supported in part by the Natural Sciences and Engineering Research Council of Canada under Grants OGP0007239, OGP0042444 and STR0117819 and in part by Optimization Systems Associates Inc.

I. INTRODUCTION

We present new theory and results applicable to circuit optimization with accurate electromagnetic (EM) simulations driven by powerful gradient-based optimizers. We go far beyond the prevailing use of stand alone EM simulators, namely, validation of designs obtained using empirical circuit models. We embark on the feasibility of efficient, automated EM optimization applicable to arbitrary geometries. Feasibility of performance-driven and yield-driven circuit optimization employing EM simulations has already been shown in previous pioneering work [1,2]. The main focus of this paper is a fundamental, new theory which we call space mapping (SM).

The hierarchy of models to choose from includes: simplified continuous models, detailed continuous models, discrete coarse models, discrete fine models and, finally, actual hardware measurements. The continuous or analytical/empirical models usually employ circuit theory and the discrete models are based on EM field theory. In general, the former models are easy to use and efficient, but may lack the necessary accuracy. The latter models are more complex and expensive but significantly more accurate. They are also applicable to general geometries. Thus, when deciding on a model, the designer must consider the existence, complexity, accuracy, cost and time associated with each model. Also, different models could be used at different stages of the design process.

In this paper we concentrate on a mathematical link between the discrete coarse and the discrete fine EM field models. However, the technique is applicable between any set of models in the hierarchy. Simulation times using EM simulators can be significantly reduced if the coarse model is more frequently used. This may decrease the accuracy of EM analysis but qualitative, and often quite accurate quantitative, information about the behaviour of the circuit can be exploited. The coarse model allows us to explore different optimization starting points, solution robustness, local minima, parameter sensitivities and statistics, and other design characteristics within a practical time frame. As design data accumulates we can analytically correlate the coarse model with the more accurate fine model.

We introduce the SM technique to direct the bulk of CPU intensive optimization to the inexpensive coarse model while preserving the accuracy and confidence offered by the fine model. The SM optimization technique requires very few fine model simulations needed in the design process. SM is a general approach and can be used to correlate other models in the hierarchy, including hardware measurements. In [3], an advanced implementation of this concept is described in the design of a high-temperature superconducting quarter-wave parallel coupled-line microstrip filter. There, an EM model is used as the fine model and an analytical/empirical circuit equivalent as the "coarse" model.

To show the benefits of coarse modeling, we carry out nominal optimization of a 3-section microstrip impedance transformer [4]. We verify the design with the fine model.

To illustrate the SM technique, we perform SM nominal optimization of a double folded stub filter [5] using the coarse model and verify the results with the fine model. Encouraged by good consistency of the results we use the coarse model to perform the otherwise very CPU demanding analysis of robustness of our optimized solution. Subsequently, we proceed with SM yield optimization of the filter. For comparison, we perform direct fine model yield optimization. In our work we utilize the OSA90/hope optimization environment [6] with the Empipe [7] interface to the *em* field simulator from Sonnet Software [8].

In Section II we explore the theory of our new SM technique. In Section III we demonstrate the use of coarse modeling and fine model verification in designing a 3-section microstrip impedance transformer. Section IV illustrates the SM technique applied to the design of a double folded stub filter. Sections V and VI contain results of coarse model robustness and SM yield optimization analyses of the double folded stub filter, respectively. Section VII describes some implications and uses of the SM optimization technique. Finally, Section VIII contains our conclusions.

II. THEORY

Consider an optimization problem for a given set of design specifications. The behaviour of the system may be described by two distinct models, namely, the coarse model and the fine model.

Let us define a k-dimensional vector of coarse model parameters as

$$\boldsymbol{\phi}_c = \left[\phi_{c1}\ \phi_{c2}\ \cdots\ \phi_{ck}\right]^T \tag{1}$$

and an l-dimensional vector of fine model parameters as

$$\boldsymbol{\phi}_f = \left[\phi_{f1}\ \phi_{f2}\ \cdots\ \phi_{fl}\right]^T. \tag{2}$$

Also, let $\boldsymbol{R}_f(\boldsymbol{\phi}_f)$ denote the fine model response at $\boldsymbol{\phi}_f$. This response is assumed to be accurate but expensive to obtain. Similarly, let $\boldsymbol{R}_c(\boldsymbol{\phi}_c)$ denote the coarse model response at $\boldsymbol{\phi}_c$. This response is generally less accurate but faster to compute.

We assume that there exists a transformation

$$\boldsymbol{\phi}_c = \boldsymbol{P}(\boldsymbol{\phi}_f) \tag{3}$$

mapping the fine model parameter space to the coarse model parameter space such that

$$\| \boldsymbol{R}_c(\boldsymbol{\phi}_c) - \boldsymbol{R}_f(\boldsymbol{\phi}_f) \| \leq \epsilon \tag{4}$$

within some local modelling region around the optimal coarse model solution $\boldsymbol{\phi}_c^*$, where ϵ is some small tolerance. Though not necessary, it is desirable that $\boldsymbol{P}$ is invertible. If so, once the transformation in (3) is found, the inverse transformation

$$\boldsymbol{\phi}_f = \boldsymbol{P}^{-1}(\boldsymbol{\phi}_c^*) \tag{5}$$

is used to find the corresponding optimal fine model solution $\boldsymbol{\phi}_f^*$ which is the image of $\boldsymbol{\phi}_c^*$ subject to (4).

Finding $\boldsymbol{P}$ is an iterative process. We begin with a set of base points $\boldsymbol{B}_f = \{ \boldsymbol{\phi}_f^1, \boldsymbol{\phi}_f^2, \ldots, \boldsymbol{\phi}_f^m \}$. The initial m base points are selected in the vicinity of the coarse model solution $\boldsymbol{\phi}_c^*$. For example, the set $\boldsymbol{B}_f$ can be chosen as $\boldsymbol{\phi}_f^1 = \boldsymbol{\phi}_c^*$ and some "reasonable" perturbations around $\boldsymbol{\phi}_f^1$. Once the set $\boldsymbol{B}_f = \{ \boldsymbol{\phi}_f^i \}$ for $i = 1, 2, \ldots, m$ is established, we evaluate the fine model responses $\boldsymbol{R}_f(\boldsymbol{\phi}_f^i)$ for $i = 1, 2, \ldots, m$. Next, we find, by parameter extraction, a set of corresponding coarse model base

points $B_c = \{ \phi_c^1, \phi_c^2, \ldots, \phi_c^m \}$ such that (4) holds. At this point, using our initial set of base points, we find P_1. At the jth iteration there are m_j base points in both sets which are used to find P_j.

Thus, at the jth iteration, to check if P_j is the desired P, we compute $\phi_f^{m_j+1}$ using the inverse transformation P_j^{-1}

$$\phi_f^{m_j+1} = P_j^{-1}(\phi_c^*) \tag{6}$$

and evaluate $R_f(\phi_f^{m_j+1})$. If

$$\| R_f(\phi_f^{m_j+1}) - R_c(\phi_c^*) \| \leq \epsilon \tag{7}$$

then $\phi_f^{m_j+1}$ is the fine model image of ϕ_c^* and we have found the transformation $P = P_j$. If (7) does not hold, we expand B_f by $\phi_f^{m_j+1}$ and B_c by the extracted $\phi_c^{m_j+1}$ subject to (4). Using the new bases B_f and B_c, P_{j+1} is found. This procedure is repeated until (7) holds. Once P is established, ϕ_f^* is taken as the image of ϕ_c^*. Fig. 1 shows a schematic describing the flow of operations of this procedure.

The key idea behind the SM optimization technique is the generation of an appropriate transformation P to map the fine model parameter space ϕ_f to the coarse model parameter space ϕ_c. To this end, we define each of the transformations P_j as a linear combination of some predefined and fixed fundamental functions

$$f_1(\phi_f),\ f_2(\phi_f),\ f_3(\phi_f),\ \ldots,\ f_n(\phi_f) \tag{8}$$

as

$$\phi_{ci} = \sum_{s=1}^{n} a_{is} f_s(\phi_f) \tag{9}$$

or, in matrix form

$$\phi_c = P_j(\phi_f) = A_j f(\phi_f) \tag{10}$$

where A_j is a $k \times n$ matrix and $f(\phi_f)$ is an n-dimensional vector of the fundamental functions and $m_j \geq n$. Consider the mapping P_j for all points in the bases B_f and B_c. We have

$$\left[\phi_c^1\ \phi_c^2\ \ldots\ \phi_c^{m_j} \right] = A_j \left[f(\phi_f^1)\ f(\phi_f^2)\ \ldots\ f(\phi_f^{m_j}) \right]. \tag{11}$$

Defining

$$\boldsymbol{C} = \left[\boldsymbol{\phi}_c^1 \ \boldsymbol{\phi}_c^2 \ \ldots \ \boldsymbol{\phi}_c^{m_j} \right]^T \tag{12}$$

and

$$\boldsymbol{D} = \left[f(\boldsymbol{\phi}_f^1) \ f(\boldsymbol{\phi}_f^2) \ \ldots \ f(\boldsymbol{\phi}_f^{m_j}) \right]^T \tag{13}$$

equation (11), augmented by some weighting factors defined by an $m_j \times m_j$ diagonal matrix $\boldsymbol{W}$

$$\boldsymbol{W} = diag(w_i) \tag{14}$$

can be rewritten as

$$\boldsymbol{W}\boldsymbol{D}\boldsymbol{A}_j^T = \boldsymbol{W}\boldsymbol{C} . \tag{15}$$

The least-squares solution to this system is

$$\boldsymbol{A}_j^T = \left(\boldsymbol{D}^T\boldsymbol{W}^T\boldsymbol{W}\boldsymbol{D} \right)^{-1} \boldsymbol{D}^T\boldsymbol{W}^T\boldsymbol{W}\boldsymbol{C} . \tag{16}$$

The SM optimization process is illustrated graphically in Fig. 2. We obtained an initial coarse model solution $\boldsymbol{\phi}_c^*$, followed by 5 additional perturbations around $\boldsymbol{\phi}_c^*$. Parameter extraction was carried out on all 6 fine model points to generate 6 corresponding coarse model base points. Using this base, a transformation was found and used to generate the next fine model base point $\boldsymbol{\phi}_f^7$. This point did not satisfy condition (7), and so the corresponding coarse model point $\boldsymbol{\phi}_c^7$ was extracted. Using this new base, another fine model point $\boldsymbol{\phi}_f^8$ was obtained from a new transformation. This point satisfied condition (7) and thus, the transformation was found.

III. NOMINAL OPTIMIZATION OF A 3-SECTION MICROSTRIP TRANSFORMER

We consider the design of a 3-section microstrip impedance transformer, shown in Fig. 3 [2,4]. The source and load impedances are 50 and 150 Ω, respectively. The design specifications imposed on the magnitude of the input reflection coefficient are as follows.

$$|S_{21}| \leq 0.11 \qquad \text{for} \qquad 5 \text{ GHz} < f < 15 \text{ GHz}$$

The error functions are calculated at frequencies from 5 GHz to 15 GHz with a 0.5 GHz step. The substrate is taken as 0.635 mm thick with relative dielectric constant of 9.7. The widths of the

transformer sections, W_1, W_2 and W_3, are considered as optimization variables. The lengths, L_1, L_2 and L_3, are kept fixed.

We perform the minimax design using a coarse model. The x and y grid sizes for the numerical EM simulation are chosen as $\Delta x_C = \Delta y_C = 0.05$ mm. 25 CPU minutes on a Sun SPARCstation 10 are needed to simulate the transformer at an arbitrary point. This includes automatic response interpolation carried out to accommodate off-the-grid geometries. To verify the coarse model design we perform fine model simulation at the coarse model minimax solution. The fine model uses a grid size of $\Delta x_F = \Delta y_F = 0.01$ mm. The fine model verification needed about 3 days.

Fig. 4 shows the $|S_{21}|$ responses of the transformer at the coarse model nominal design together with the fine model verification. It can be seen that the coarse model response closely approximates the fine model response. Clearly, the coarse model can be used for fast analysis of general performance characteristics and exploration of a good starting point for fine model or SM optimization. Fig. 5 shows the coarse model response at the nominal solution once more but this time together with responses at four on-the-grid points used to approximate the response at the off-the-grid nominal point. This necessary geometrical interpolation, requires a significant amount of CPU time, especially if the fine model is used. In contrast, the SM technique can be carried out *without any interpolation* of the fine model.

IV. COARSE MODEL AND SM OPTIMIZATION OF THE DOUBLE FOLDED STUB FILTER

We optimize the double folded stub filter of Fig. 6. The x and y grid sizes for the coarse model simulation are chosen as $\Delta x_C = \Delta y_C = 4.8$ mil. The fine model simulation used to verify the coarse model results use grid sizes of $\Delta x_F = \Delta y_F = 1.6$ mil. The three designable parameters are L_1, L_2 and S. Parameters W_1 and W_2 are fixed at 4.8 mil each. The design specifications are

$$|S_{21}| \geq -3 \text{ dB} \quad \text{for} \quad f \leq 9.5 \text{ GHz and } f \geq 16.5 \text{ GHz}$$

$$|S_{21}| \leq -30 \text{ dB} \quad \text{for} \quad 12 \text{ GHz} \leq f \leq 14 \text{ GHz}.$$

For the coarse model case, the time needed to simulate the filter at a single frequency and an arbitrary point is about 5 CPU seconds. This includes automatic response interpolation carried out to accommodate off-the-grid geometries. The corresponding time for the fine model is approximately 70 seconds on a Sun SPARCstation 10. The coarse model minimax solution is listed in Table I. The $|S_{21}|$ response of the filter before and after coarse model minimax optimization is shown in Fig. 7.

The corresponding fine model response does not satisfy the design specifications. To further refine the fine model solution we applied our new SM optimization technique. The main advantage of the SM method is that it requires very few fine model simulations. The refined SM solution is listed in Table I. Fig. 8 shows the $|S_{21}|$ response at the coarse model minimax solution and at the refined SM solution both simulated with the fine model. Fig. 9 shows the $|S_{21}|$ match between the coarse model minimax solution simulated using the coarse model and its image, the SM solution simulated using the fine model. The SM technique needed in total eight fine model simulations to establish a mapping with the resulting match as shown in Fig 9. Tables II and III list the fine and coarse model base points used. In the parameter extraction phase, various optimizers including the ℓ_1, ℓ_2 and the novel Huber [9] optimizer were used to ensure a good match. In this implementation, a subjective criterion based on appearance was used to determine the "goodness" of the fit between the two responses. Fig. 10 illustrates the parameter extraction process showing the match before and after parameter extraction for a pair of base points.

Comparing the responses in Figs. 7 and 8 shows that the coarse model can very closely approximate responses obtained using the much more CPU intensive fine model. Design using the coarse model can then be followed, if necessary, by applying SM or direct fine model optimization, to further refine the fine model solution. The latter is not recommended.

V. ROBUSTNESS ANALYSIS OF THE NOMINAL SOLUTION

For the double folded stub filter we want to investigate the robustness of the coarse model nominal solution. We select the same optimization variables, namely, L_1, L_2 and S as in the

nominal minimax design. W_1 and W_2 are kept fixed. Subsequently, we perform a number of coarse model minimax optimizations, each starting from a different random starting point. We use 30 different starting points uniformly spread around the minimax solution within a ±20% deviation.

Fig. 11(a) plots the $|S_{21}|$ responses for all 30 starting points. Bars in Fig. 11(b) represent the Euclidian distances between the minimax solution and the perturbed starting points. Fig. 12 shows the corresponding diagrams after minimax optimizations. In Fig. 13, we visualize the optimization trajectories taken by the minimax optimizer by showing lines identifying corresponding starting points with optimized solutions for each optimization. These lines are shown for different pairs of designable parameters.

We can observe that nearly all of the optimizations converged to the reference minimax solution. This shows that the optimized nominal solution is robust and that coarse model optimization provides consistent results even if started from different starting points. This study has been confirmed from other families of starting points and with other gradient optimizers. To perform similar analysis with the fine model would be prohibitively long.

VI. YIELD OPTIMIZATION OF THE DOUBLE FOLDED STUB FILTER

For Monte Carlo estimation we assume a uniform distribution with 0.25 mil tolerance on all five geometrical parameters. Yield optimization is performed using the techniques and within the environment described in [2]. The optimizable parameters are L_1, L_2 and S, with W_1 and W_2 fixed at 4.8 mil each.

Monte Carlo yield estimated from 250 outcomes using the 4.8 mil coarse model at the coarse model nominal minimax solution is 71%. After coarse model yield optimization using 200 outcomes, the estimated yield is increased to 81%. Subsequently, we performed yield estimation utilizing the 1.6 mil fine model at the coarse model nominal and centered solutions. The fine model estimated yields are both 0%. This shows the potential pitfalls of relying on coarse model-only design. Fig. 14(a) shows the fine model simulated $|S_{21}|$ Monte Carlo sweep at the coarse model centered solution.

Utilizing the SM transformation built to find the nominal SM solution we performed yield analysis. The yield estimated from 250 statistical outcomes using the 1.6 mil fine model at the SM nominal solution is 9%. After carrying out yield optimization for 200 outcomes, utilizing the forward SM transformation, the yield increased to 24%. This result is compared with direct fine model yield optimization, which produced a comparable centered yield of 30%. Fig. 13(b) shows the fine model simulated $|S_{21}|$ Monte Carlo sweep at the forward SM transformed centered solution. Both solutions are listed in Table IV.

Subsequently, we perform Monte Carlo analyses utilizing the 1.6 mil fine model at the nominal and centered solutions using relaxed design specifications. Two cases are considered. For case (a), both the upper and lower specifications are relaxed by 0.5 dB. For case (b), both specifications are relaxed by 1 dB. Both updated centered yields are listed in Table V. They show remarkable similarity.

VII. CONCLUSIONS

We have presented a new theory describing a novel SM optimization technique, a competitive alternative to traditional optimization. The SM approach exploits the speed of an efficient model and blends it with a few expensive but highly accurate model evaluations to effectively perform nominal and yield optimization. In this presentation we use coarse and fine EM models as the efficient but less accurate and, less efficient but much more accurate models, respectively. In general however, the SM technique can correlate any two from a hierarchy of available models including, hardware measurements. The SM mapping technique is especially attractive when used with CPU intensive simulators since it requires only a few simulations in the entire design process.

We have presented results involving coarse model nominal optimization design of a 3-section microstrip impedance transformer and a double folded stub filter. For the double folded stub filter we also performed SM nominal optimization as well as coarse model and SM design centering. Fine model verifications of the optimized solutions demonstrate that coarse models can provide useful

qualitative and quantitative information about the performance of a circuit within a practical time frame.

We have also analyzed the robustness of the coarse model solution. In the examples presented we did not explore the weighting factors available in SM. The weighting factors affect the influence of corresponding base points on the SM transformation. In the double folded stub filter example the consecutive base points were located in the same region as the ones already established. But if the assumed modelling region has a tendency to move, then the weighting factors should be used in order to reduce the effect of base points located further away from the current modeling region. This study, however, is left for future investigation.

ACKNOWLEDGEMENT

The authors wish to thank Dr. K. Madsen of the Institute of Mathematical Modelling, Technical University of Denmark, Lyngby, Denmark for early discussions with the first author. Dr. J.C. Rautio of Sonnet Software, Inc., Liverpool, NY is thanked for making *em* available for this work.

REFERENCES

[1] J.W. Bandler, S. Ye, R.M. Biernacki, S.H. Chen and D.G. Swanson, Jr., "Minimax microstrip filter design using direct EM field simulation," *IEEE MTT-S Int. Microwave Symp. Dig.* (Atlanta, GA), 1993, pp. 889-892.

[2] J.W. Bandler, R.M. Biernacki, S.H. Chen, P.A. Grobelny and S. Ye, "Yield-driven electromagnetic optimization via multilevel multidimensional models," *IEEE Trans. Microwave Theory Tech.*, vol. 41, 1993, pp. 2269-2278.

[3] J.W. Bandler, R.M. Biernacki, S.H. Chen, P.A. Grobelny, C. Moskowitz and S.H. Talisa, "Electromagnetic design of high-temperature superconducting microwave filters," *IEEE MTT-S Int. Microwave Symp.*, (San Diego, CA), 1994.

[4] J.W. Bandler, R.M. Biernacki, S.H. Chen and P.A. Grobelny, "A CAD environment for performance and yield driven circuit design employing electromagnetic field simulators," *Proc. Int. Symp. Circuits and Systems*, (London, England), 1994.

[5] J.C. Rautio, Sonnet Software, Inc., 135 Old Cove Road, Suite 203, Liverpool, NY 13090-3774, Private communication, 1992.

[6] *OSA90/hope™*, Optimization Systems Associates Inc., P.O. Box 8083, Dundas, Ontario, Canada L9H 5E7, 1993.

[7] *Empipe™*, Optimization Systems Associates Inc., P.O. Box 8083, Dundas, Ontario, Canada L9H 5E7, 1993.

[8] *Em User's Manual*, Sonnet Software, Inc., 135 Old Cove Road, Suite 203, Liverpool, NY 13090-3774, 1992.

[9] J.W. Bandler, S.H. Chen, R.M. Biernacki, L. Gao, K. Madsen, H. Yu, "Huber optimization of circuits: a robust approach," *IEEE Trans. Microwave Theory Tech.*, vol. 41, 1993, pp. 2279-2287.

TABLE I
NOMINAL DESIGN OPTIMIZATION

Parameter (mil)	Before Optimization	Coarse Grid Solution	SM Refined Solution
L_1	90.0	91.5	93.7
L_2	80.0	85.7	85.3
S	4.8	4.1	4.6

W_1 and W_2 are kept fixed at 4.8 mil.

TABLE II
FINE MODEL BASE POINTS

Base Point	L_1	L_2	L_3
ϕ_f^1	91.482	85.735	4.139
ϕ_f^2	96.056	85.735	4.139
ϕ_f^3	91.482	90.021	4.139
ϕ_f^4	91.482	85.735	4.800
ϕ_f^5	86.908	85.735	4.139
ϕ_f^6	86.908	81.448	4.800
ϕ_f^{7*}	93.981	85.324	4.579
ϕ_f^{8*}	93.693	85.314	4.590

All parameters are in mils. ϕ_f^7 and ϕ_f^8 are generated from the SM transformation.

TABLE III
EXTRACTED COARSE MODEL BASE POINTS

Base Point	L_1	L_2	L_3
ϕ_c^1	86.392	86.102	4.129
ϕ_c^2	94.694	85.774	3.762
ϕ_c^3	97.242	90.854	2.791
ϕ_c^4	87.462	86.209	4.502
ϕ_c^5	85.092	86.072	3.704
ϕ_c^6	85.002	82.387	3.912
ϕ_c^7	92.096	85.701	4.163

All parameters are in mils.

TABLE IV
YIELD OPTIMIZATION

Parameter (mil)	Before Yield Optimization	SM Yield Optimization	Fine Model Yield Optimization
L_1	93.7	92.0	91.8
L_2	85.3	85.0	85.1
S	4.6	5.0	4.9
Fine Model Yield	9%	24%	30%

Uniform tolerances of 0.25 mil on all five geometrical parameters. Yield estimation based on 250 outcomes. Yield optimization using 200 outcomes.

TABLE V
FINE GRID YIELD OPTIMIZATION
FOR RELAXED CONSTRAINTS

Case	SM Nominal Yield	SM Centered Yield	Fine Model Centered Yield
(a)	63%	87%	88%
(b)	81%	97%	96%

Case (a): the lower specification is S_l = -3.5 dB and the upper specification S_u = -29.5 dB. Case (b): S_l = -4 dB, S_u = -29 dB.

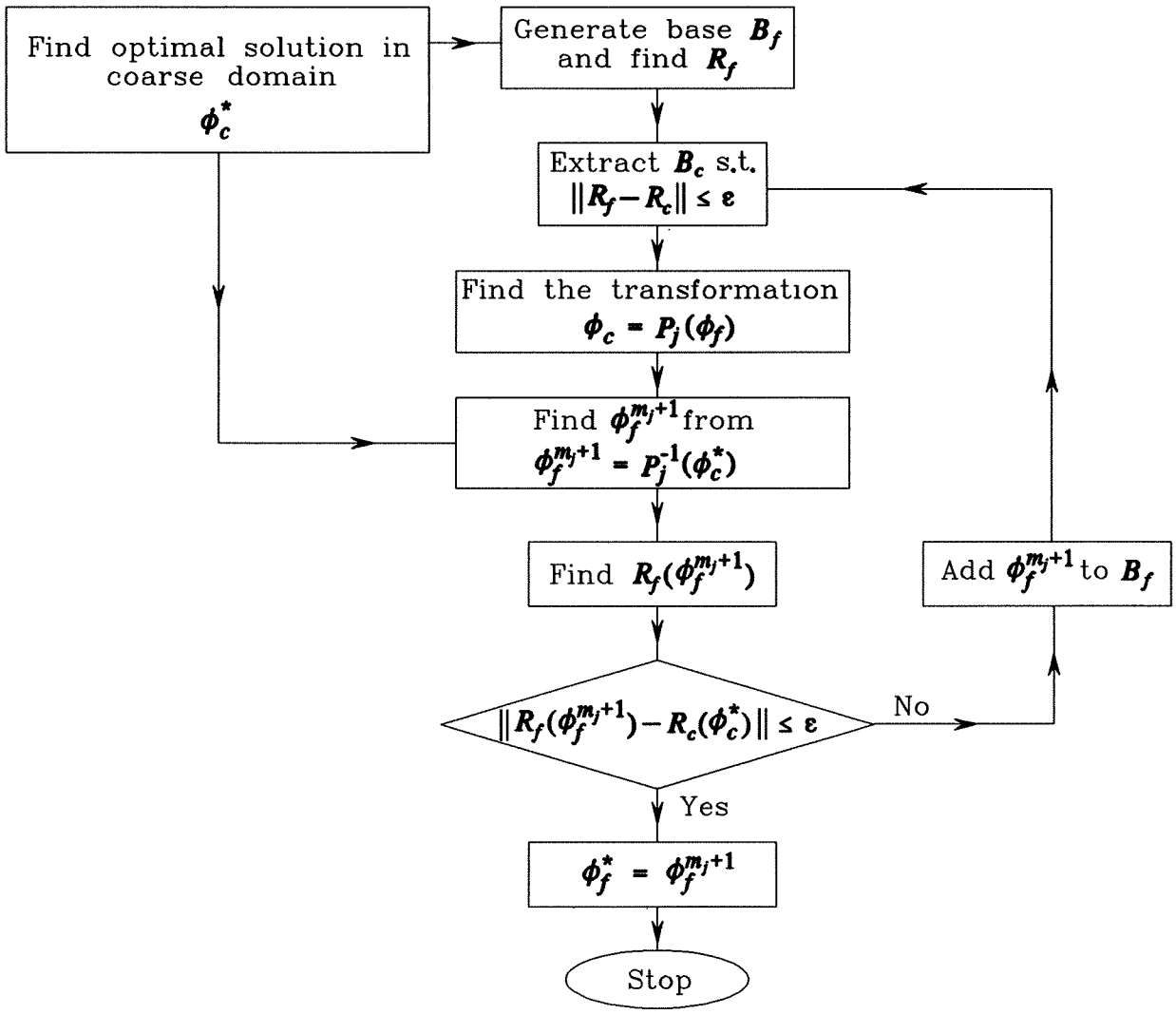

Fig. 1. Schematic diagram describing the space mapping (SM) optimization technique.

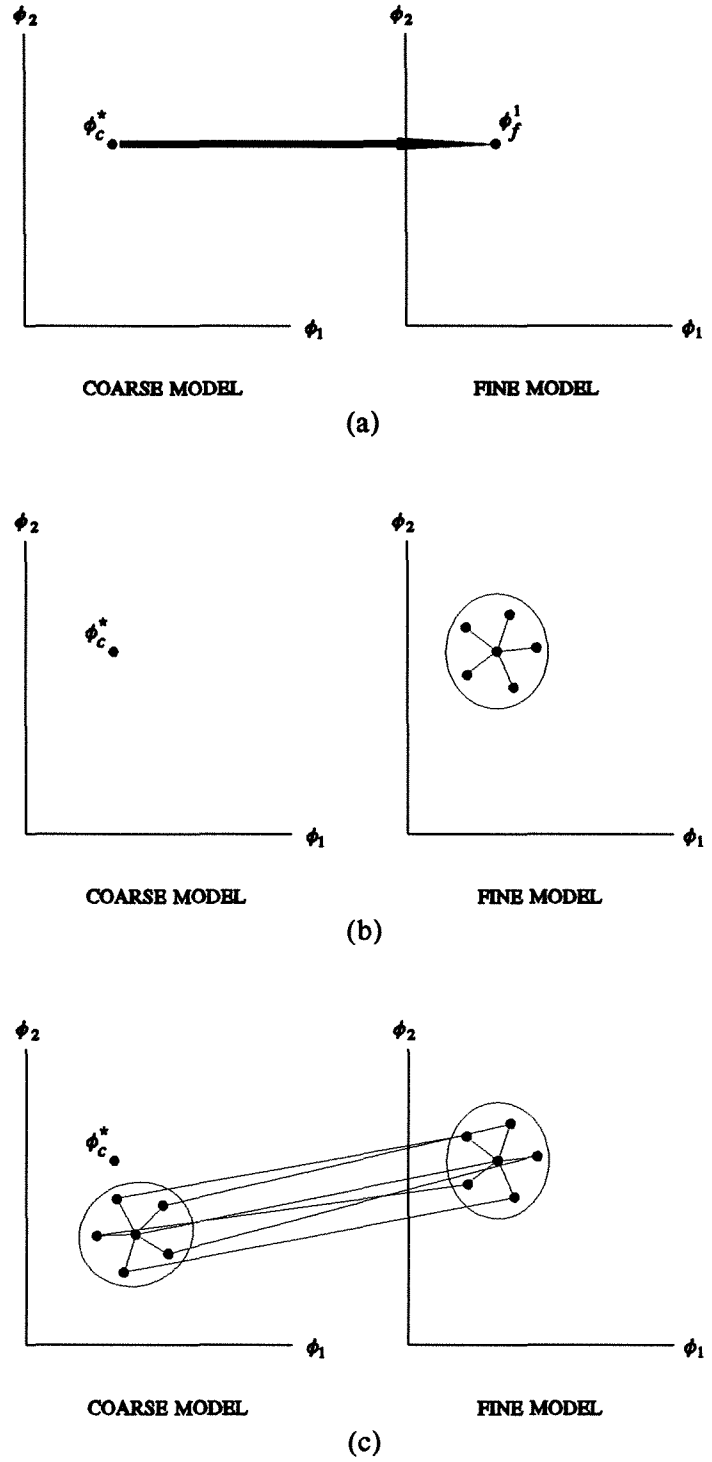

Fig. 2. Illustration of the SM process. (a) Coarse model optimization to obtain $\boldsymbol{\phi}_c^*$. (b) Generation of five additional perturbations around $\boldsymbol{\phi}_f^1 = \boldsymbol{\phi}_c^*$. (c) Perform coarse model parameter extraction to match the fine model responses.

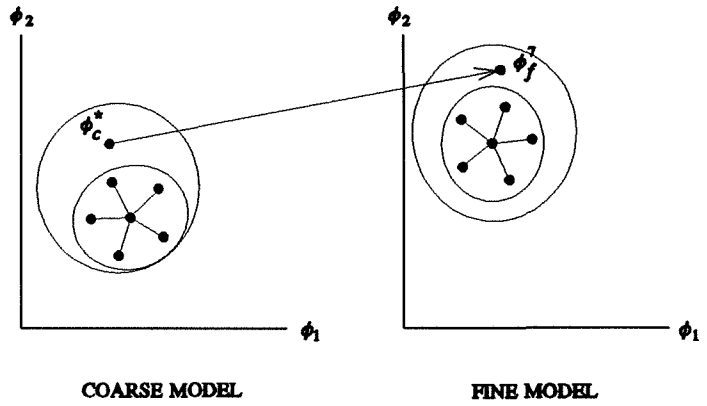

(d)

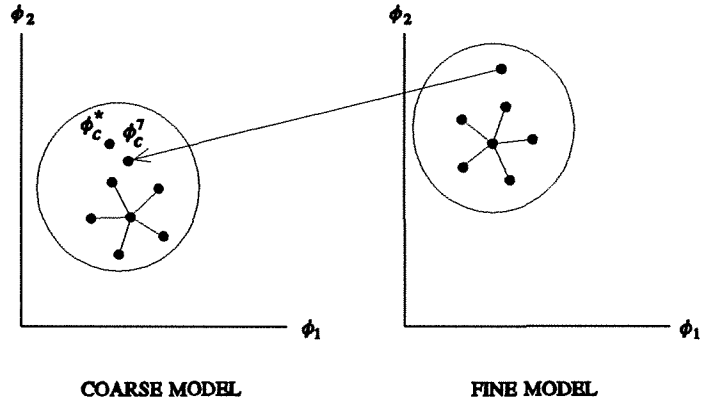

(e)

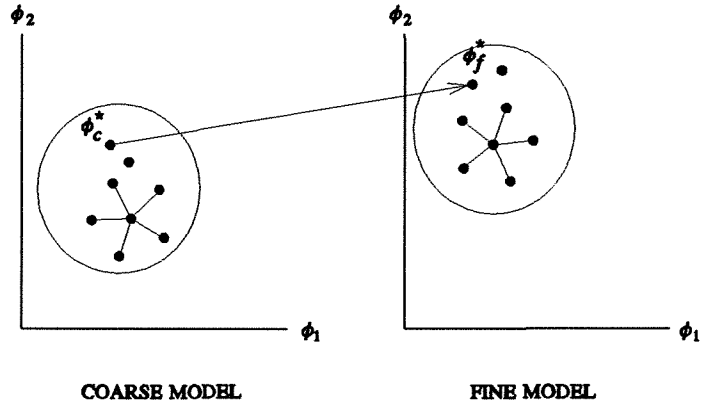

(f)

Fig. 2 (cont.) (d) Use inverse transformation to obtain the fine model point $\phi_f^{m+1} = \phi_f^7$, which in this case did not satisfy (5). (e) Perform coarse model parameter extraction again to obtain ϕ_c^7. (f) Use the new projection model to obtain $\phi_f^* = \phi_f^8$.

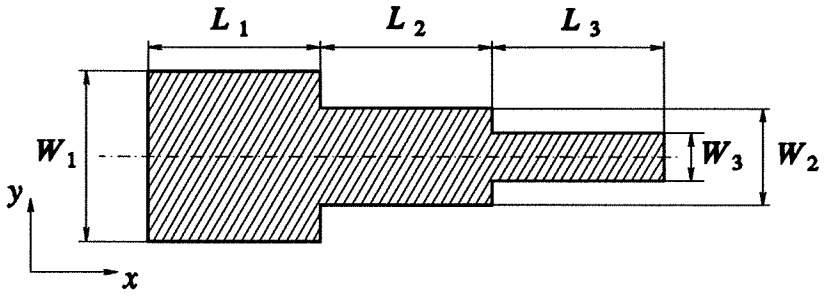

Fig. 3. 3-section microstrip impedance transformer. The widths of the sections W_1, W_2 and W_3 are the designable parameters. The lengths L_1, L_2 and L_3 are fixed.

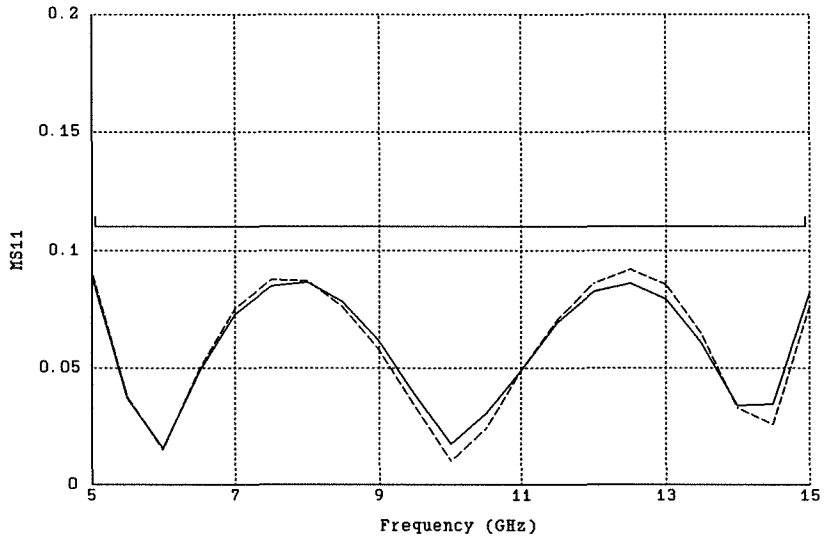

Fig. 4. Coarse model design of a 3-section microstrip impedance transformer and fine model verification. The coarse model $|S_{11}|$ response of the transformer at the minimax solution is shown as a dashed line. The corresponding fine model verification is shown as a solid line. Good agreement between the responses can be observed.

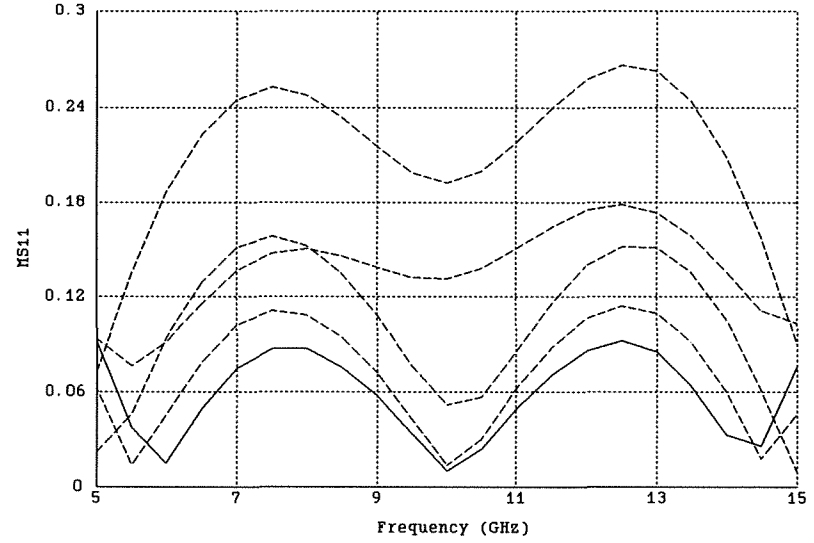

Fig. 5. Coarse model $|S_{11}|$ simulation of the 3-section microstrip impedance transformer at the off-the-grid minimax design solution (solid line). The four dashed lines represent $|S_{11}|$ responses obtained at the on-the-grid points surrounding the minimax solution point and used to approximate the responses at the minimax solution point. Fine model simulation of a typical off-the-grid point will require significant CPU time due to the necessary interpolation required to accommodate the off-the-grid points.

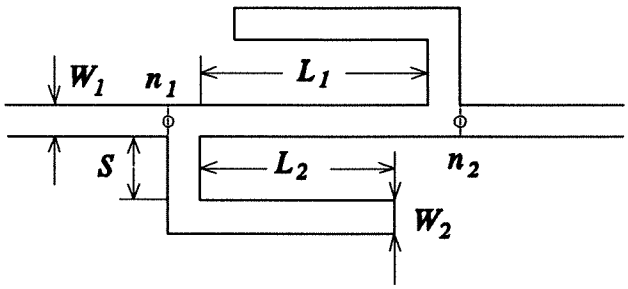

Fig. 6. Microstrip double folded stub bandstop filter [5].

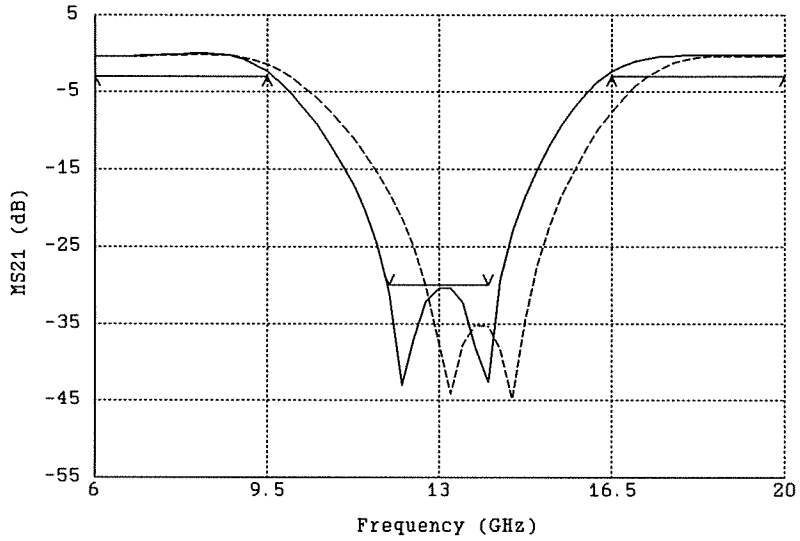

Fig. 7. Coarse model design of the double folded stub filter. The $|S_{21}|$ response of the filter before (dashed line) and after (solid line) minimax optimization as simulated by the coarse model.

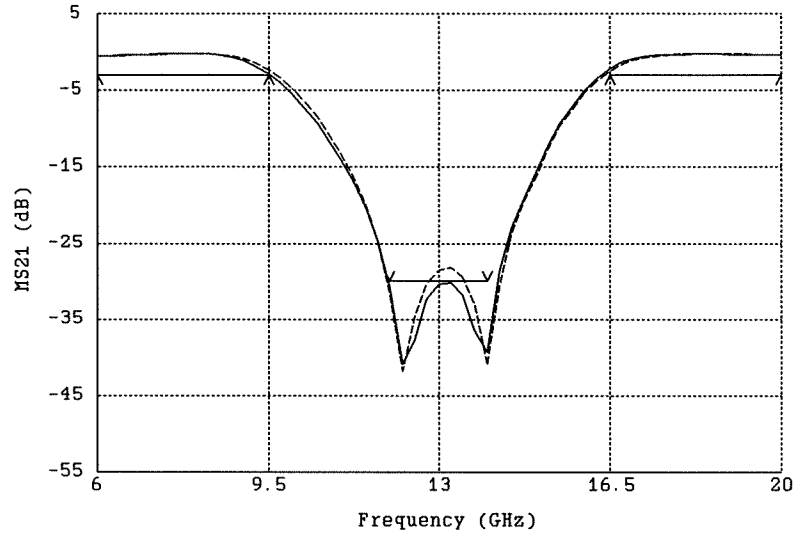

Fig. 8. Fine model design of the double folded stub filter. The $|S_{21}|$ response at the coarse model minimax solution (dashed line) and the $|S_{21}|$ response at the SM refined solution simulated (solid line). Both responses were simulated using the fine model.

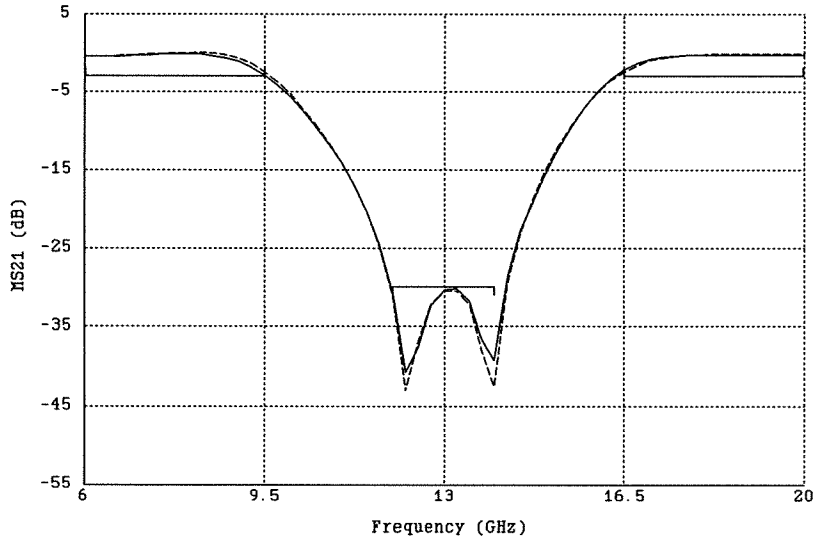

Fig. 9. SM design of the double folded stub filter. The $|S_{21}|$ response at the minimax coarse model solution as simulated using the coarse model (solid line) and the $|S_{21}|$ response at the SM refined solution as simulated using the fine model (dashed line). The responses compare very well proving high accuracy of the transformation established in the SM process.

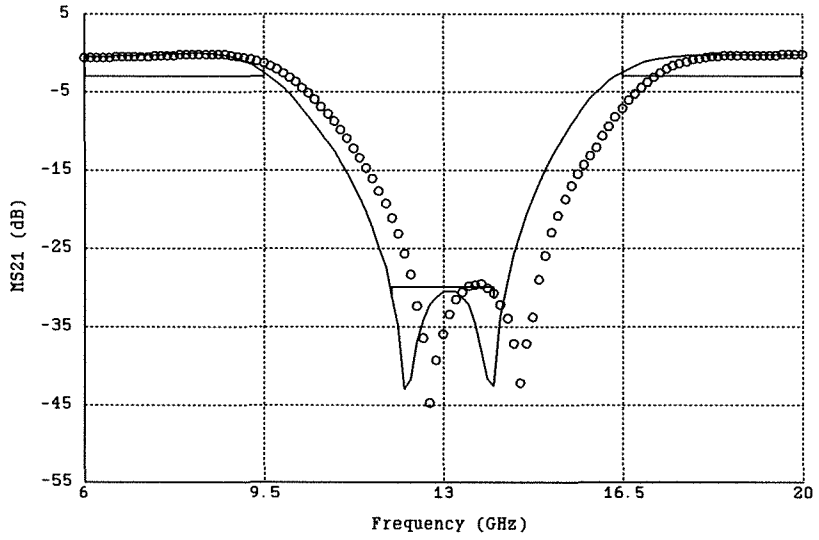

(a)

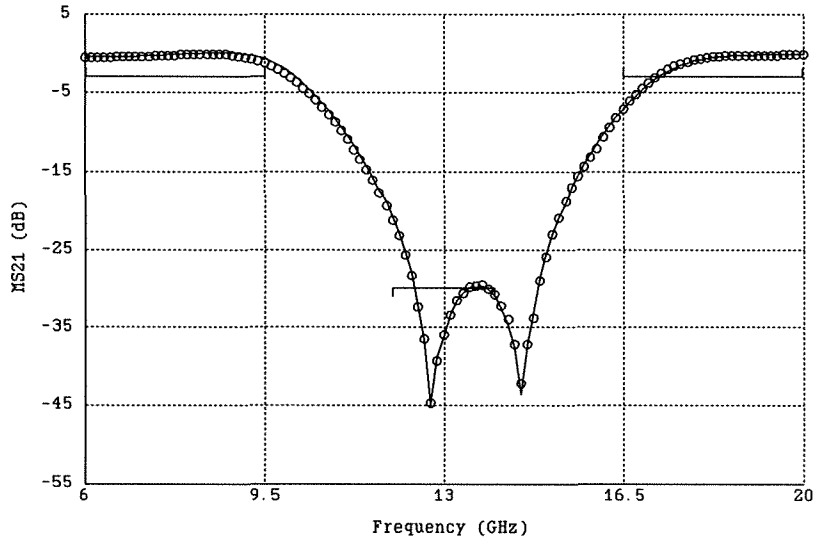

(b)

Fig. 10. Illustration of the parameter extraction process using 121 frequency points. The figure shows the $|S_{21}|$ response match for one pair of the coarse and fine model base points. (a) Match before and (b) match after parameter extraction. Fine and coarse model simulated responses are shown with circles and a solid line, respectively. The fine model uses a grid size of 1.6 mil. The coarse model uses a grid size of 4.8 mil.

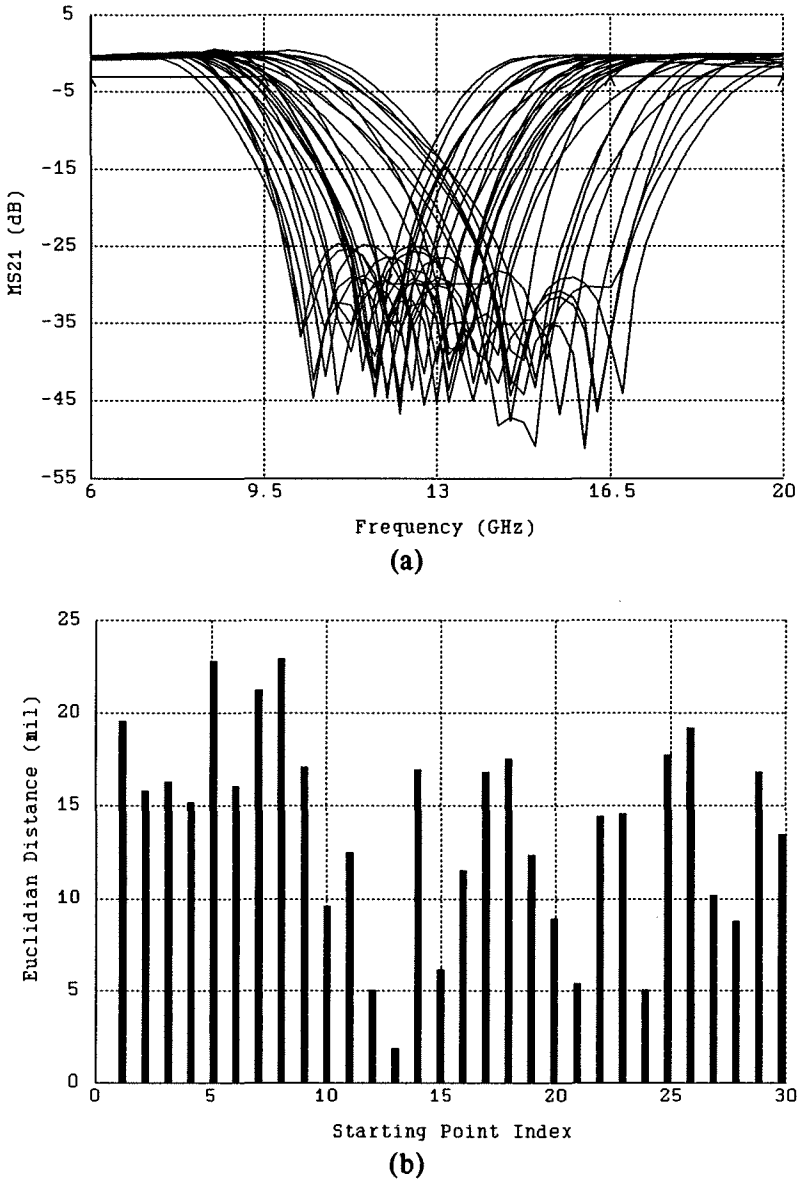

Fig. 11. Robustness analysis of the nominal solution of the double folded stub filter. (a) Coarse model simulated $|S_{21}|$ response at 30 points randomly scattered around the reference minimax solution, and (b) the Euclidian distances between the random starting points and the reference minimax solution.

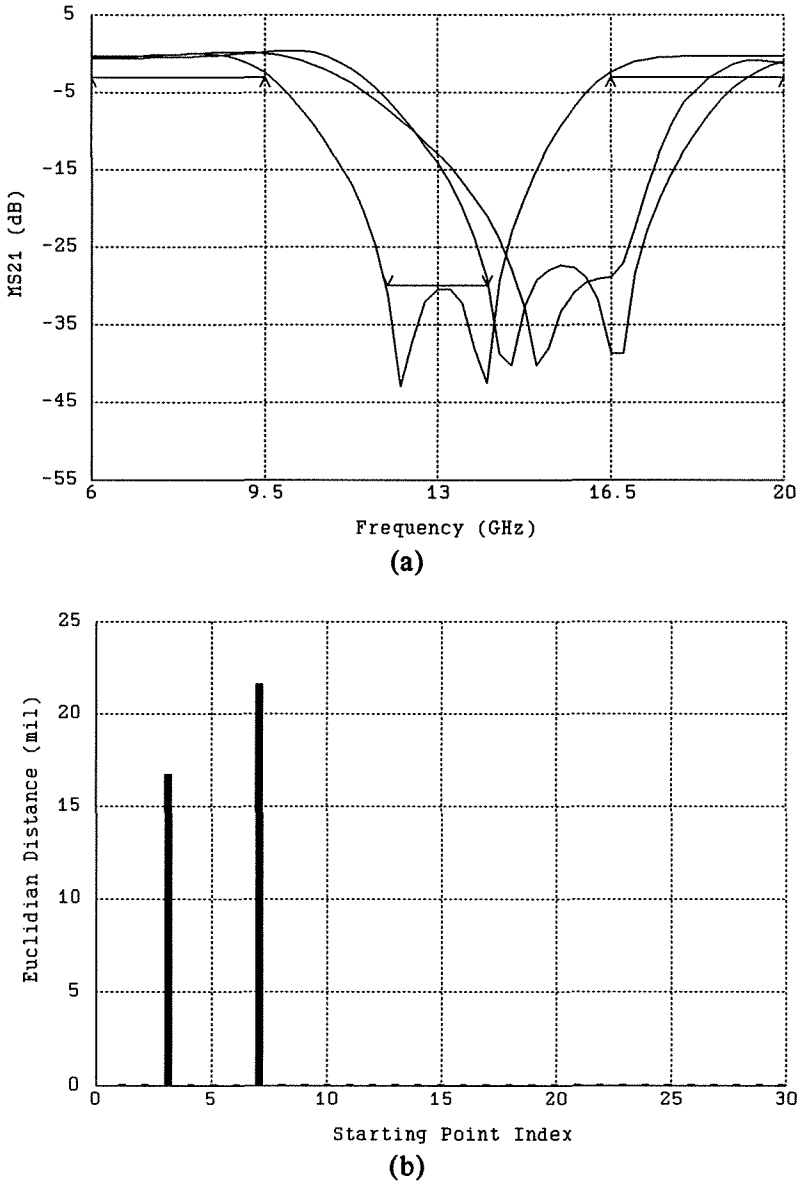

Fig. 12. Robustness analysis of the nominal solution of the double folded stub filter. (a) Coarse model simulated $|S_{21}|$ response at the optimized solutions from the 30 randomly generated starting points shown in Fig. 11. (b) the Euclidian distances between the optimized points and the reference minimax solution. Most of the optimizations converged to the original minimax solution.

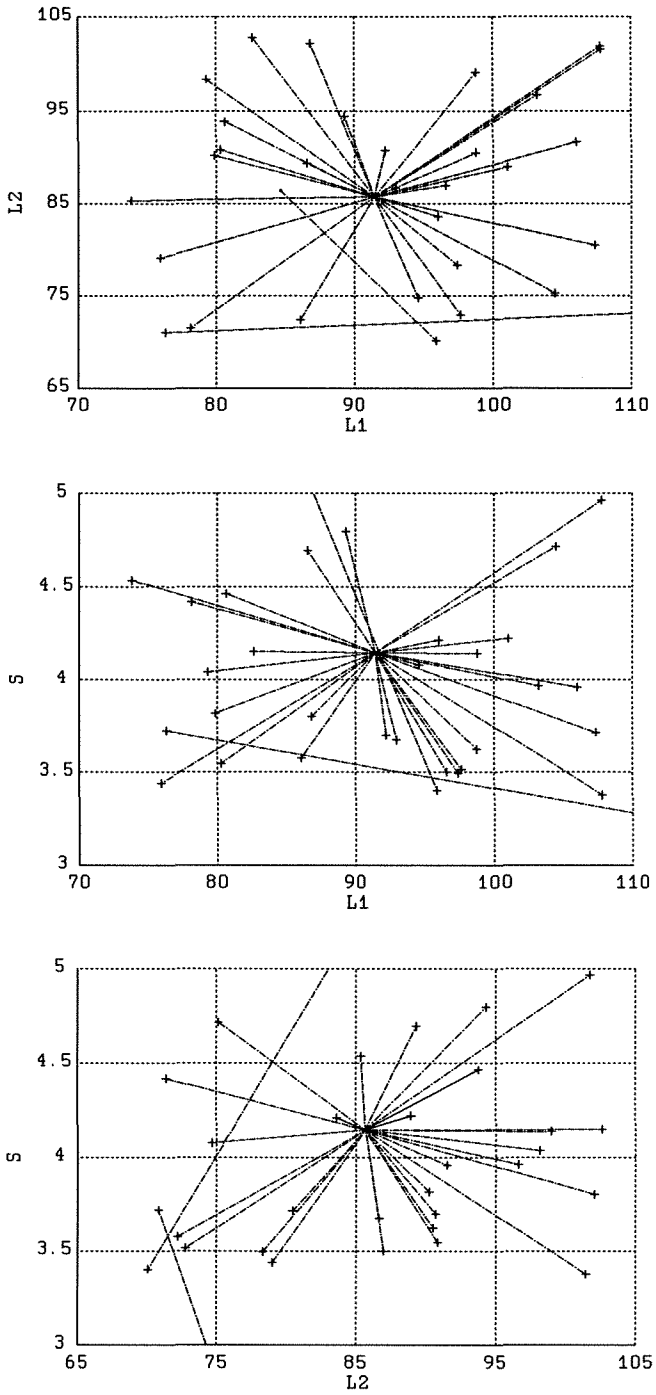

Fig. 13. Robustness analysis of the nominal solution of the double folded stub filter. Visualization of the trajectories taken by the minimax optimizer for each of the randomly generated starting points. Lines identifying corresponding starting points (+) with optimized solutions (·) for each optimization are shown in two-dimensional subspaces of the designable parameters: L_1, L_2 and S.

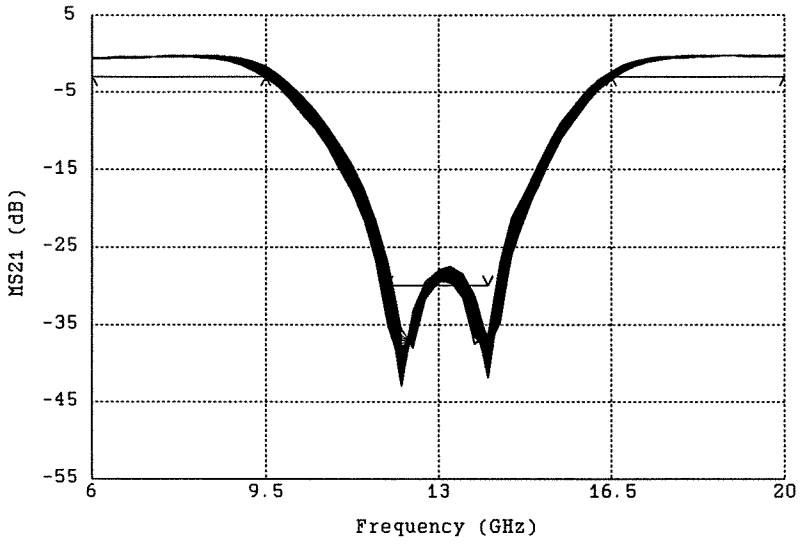

(a)

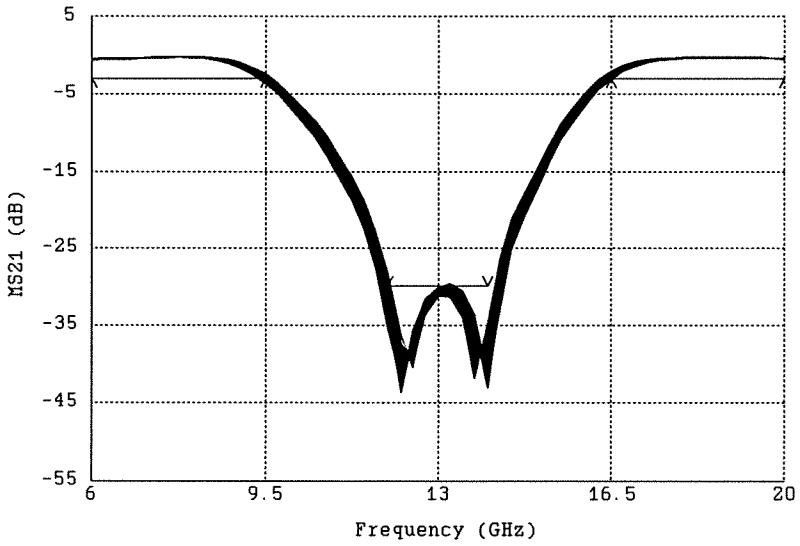

(b)

Fig. 14. The $|S_{21}|$ Monte Carlo sweep obtained using the fine model after (a) coarse model yield optimization and (b) SM yield optimization. 250 outcomes are used for yield estimation and 200 outcomes are used in yield optimization.